Journal of Nanobiotechnology

RESEARCH

Open Access

Colostrum-derived extracellular vesicles: potential multifunctional nanomedicine for alleviating mastitis

Yindi Xiong[1,3†], Taiyu Shen[1†], Peng Lou[2], Jingyue Yang[1], John P. Kastelic[3], Jingping Liu[2], Chuang Xu[1], Bo Han[1] and Jian Gao[1*]

Abstract

Bovine mastitis is an infectious disease that causes substantial economic losses to the dairy industry worldwide. Current antibiotic therapy faces issues of antibiotic misuse and antimicrobial resistance, which has aroused concerns for both veterinary and human medicine. Thus, this study explored the potential of Colo EVs (bovine colostrum-derived extracellular vesicles) to address mastitis. Using LPS-induced murine mammary epithelial cells (HC11), mouse monocyte macrophages (RAW 264.7), and a murine mastitis model with BALB/C mice, we evaluated the safety and efficacy of Colo EVs, *in vivo* and *in vitro*. Colo EVs had favorable biosafety profiles, promoting cell proliferation and migration without inducing pathological changes after injection into murine mammary glands. In LPS-induced murine mastitis, Colo EVs significantly reduced inflammation, improved inflammatory scores, and preserved tight junction proteins while protecting milk production. Additionally, *in vitro* experiments demonstrated that Colo EVs downregulated inflammatory cytokine expression, reduced inflammatory markers, and attenuated NF-κB pathway activation. In summary, we inferred that Colo EVs have promise as a therapeutic approach for mastitis treatment, owing to their anti-inflammatory properties, potentially mediated through the NF-κB signaling pathway modulation.

†Yindi Xiong and Taiyu Shen contributed equally to this work.

*Correspondence:
Jian Gao
gaojian2016@cau.edu.cn

Full list of author information is available at the end of the article

Graphical Abstract

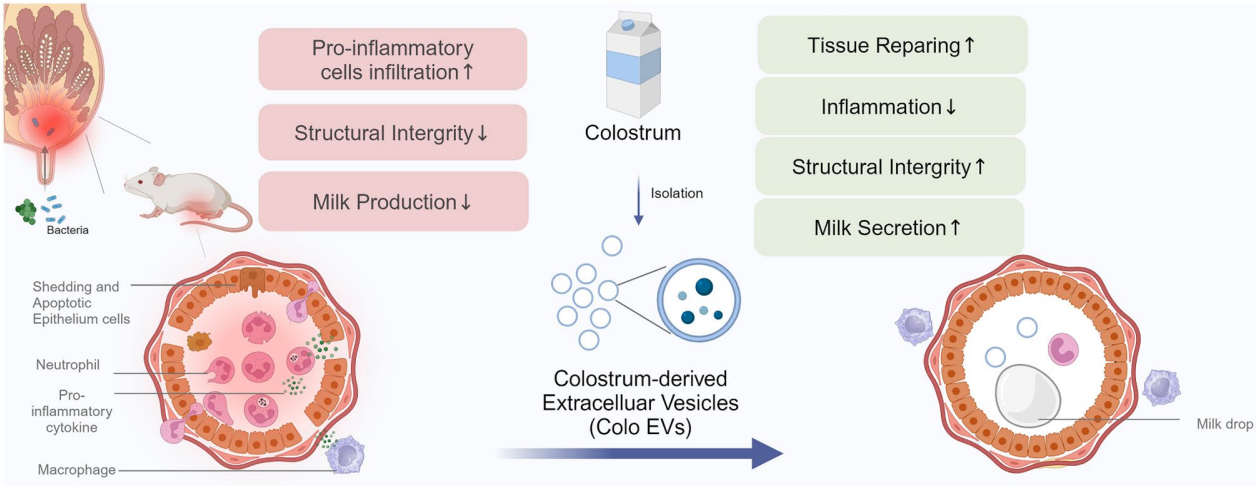

Keywords Bovine mastitis, Colostrum, Extracellular vesicles, Exosome

Introduction

Mastitis is a prevalent disease characterized by inflammation and damage in mammary glands, representing a substantial economic burden on the dairy industry worldwide [1]. As one of the most costly diseases on dairy farms, a single case of clinical mastitis will lead to ~$444 (USD) total economic loss [2], with estimates of $19.7B-32B (USD) in losses annually in the global dairy industry [3].

Bacterial infection is the primary causative factor of mastitis, triggering an excessive inflammatory response characterized by infiltration of neutrophils led by activation of macrophages into mammary tissue [4], releasing oxidative stress-related mediators, causing tissue damage and diminishing future milk production [5]. The blood-milk barrier (BMB) has a central role in mammary immunity, using tight junctions to block infiltration of immune cells and bacteria [6]. However, during mastitis, the BMB integrity is compromised, exacerbating inflammation and promoting damage [7].

Currently, the main therapeutic approach to mastitis is intramammary antibiotic injections [8]. Though antibiotics are often effective, there are drawbacks. Firstly, the abuse of antibiotics in agricultural production and the health hazards relating to antimicrobial resistance are raising awareness worldwide. Secondly, antibiotics are to inhibit or kill bacteria, but they do not alleviate inflammation or tissue damage, subsequent decreases in milk yield, or other cattle health problems, e.g. stress and reduced fertility. Thus, novel therapeutic agents for mastitis remain crucial.

Extracellular vesicles (EVs) are nanovesicles that transport signals between cells and mediate intracellular communications [9]. EVs contain rich bioactive contents inherited from parent cells, with therapeutic potential in multiple disorders including inflammation [10], tissue damage [11], and fibrosis [12]. Recently, EVs from milk have gathered attention for their high yield and safety profile [13]. However, compared to milk, colostrum contains higher concentrations of immune-active substances including cytokines, defensins, and microRNA [14, 15] and colostrum-derived EVs (Colo EVs) contain richer proteins relating to immunomodulation and growth [16]. Additionally, Colo EVs have potential anti-inflammatory and antioxidant properties, attributed to transporting bioactive molecules [17, 18].

Despite the recognized properties of Colo EVs, their impacts on mastitis remains largely unexplored. Given the important role of inflammation and BMB disruption in mastitis pathogenesis, understanding potential anti-inflammatory properties of Colo EVs and their ability to preserve BMB integrity could offer valuable insights into novel therapeutic approaches for mastitis management.

E. coli is one of the most common bacteria to cause severe clinical mastitis [19]. When LPS, a crucial virulence factor of *E. coli*, is infused intramammarily, it triggers a severe inflammatory response, with severe inflammation and mammary gland damage [20]. Therefore, this study aimed to assess whether Colo EVs exhibit anti-inflammatory properties and preserve BMB integrity in LPS-induced mastitis models.

Materials and methods

Statement of ethics

This study was conducted in compliance with guidelines of the Beijing Municipality on the Review of Welfare and

Ethics of Laboratory Animals, approved by the Beijing Municipality Administration Office of Laboratory Animals (BAOLA) and China Agricultural University Animal Ethics Committee (ID: AW11604202-2-1).

Isolation and characterization of bovine colostrum extracellular vesicles

Pasteurized bovine colostrum was obtained from a commercial dairy farm in Beijing, China. The colostrum was randomly collected from 4 multiparous Holstein cows with no disease records during the dry-off period. Colostrum was collected in the first lactation (within 12 h) after calving. It was heated to 60 °C for 60 min, following standard farm procedures.

To eliminate milk fat, 30 mL colostrum underwent centrifugation at 5,000 × g for 30 min and subsequently at 13,000 × g for an additional 30 min, both at 4 ℃ (Eppendorf 5810R, Germany). The defatted milk was then diluted eightfold in phosphate-buffered saline (PBS). Ultracentrifugation was performed with an SW32Ti rotor at 100,000 × g for 60 min at 4 ℃ (Beckman/Optima XPN-100), and the resulting sediment was retained and supernatant discarded. Subsequently, the sediment was subjected to centrifugation at 135,000 × g at 4 ℃ for 70 min. The sediment was washed under the same conditions. The sediment, recognized as Colo EVs, was resuspended in 10 mL of sterile PBS using a centrifuge. The suspension was then passed through a 100 kDa Ultra Centrifugal filter (Sigma, UFC910008, USA) to obtain a purified EV sample. Pure EV pellets were resuspended in PBS and stored at -80 ℃ pending use. Supernatant was centrifuged at 175,000 × g at 4 ℃ for 60 min and frozen for further use.

Transmission electron microscopy (TEM)

The Colo EVs were fixed and transmission electron microscopy was used to assess ultrastructure. Briefly, 10 μL of Colo EVs suspension was carefully deposited onto parafilm, and formvar-coated copper grids (Electron Microscopy Sciences, USA) were gently placed on the drops, ensuring the coated side facing the suspension. Colo EVs were allowed to adhere to the grids for approximately 20 min. Grids were subsequently contrasted with 2% uranyl acetate for 5 min following a thorough rinse in PBS and distilled water. Images were obtained by a transmission electron microscope (H7650, Hitachi, Tokyo, Japan) at an accelerating voltage of 80 kV.

Nanoparticle tracking analysis (NTA)

The size distribution of Colo EVs was measured by a nanoparticle tracking analyzer (NTA, Particle Metrix, Meerbusch, Germany) used to assess Brownian motion of EVs suspended in PBS, and size distribution data were generated by applying the Stokes-Einstein equation. Concentration and diameter results are reported as mean ± standard error of the mean.

Cell culture and treatment

The HC11 murine mammary epithelial cell line (ATCC, USA) was generously provided by Prof. Chuang Xu from China Agricultural University. The RAW 264.7 mouse monocyte macrophage origin cells were purchased from Procell Co. Ltd, China and cultured in Dulbecco's modified Eagle medium (DMEM; Gibco, USA) supplemented with 10% fetal bovine serum (Gibco, USA) in a T25 culture flask (Corning, USA) incubated in 5% CO_2 at 37 ℃. Cells were sub-cultured when they reached 80 to 90% confluence.

RAW264.7 were seeded at 6-well plates with 10% FBS culture medium at a density of ~10^5 cells/mL per well and cells allowed to attach overnight. Colo EVs (10 and 20 μg/mL) and supernatant (50 μg/mL) were added to the culture medium. Thirty minutes after addition of Colo EVs, the medium was gently removed and washed with new medium. Then,1 μg/mL LPS (L2880, from E. coli O55:B5, Sigma-Aldrich, USA) was added to to the culture medium and after 12 h, cells were collected.

The HC11 cells were seeded in 6-well plates with 10% FBS medium until the cell reached 80% confluence and then replaced with 2% FBS media. Colo EVs (40 and 50 μg/mL) were added to culturing wells and 30 min later, the medium was gently removed and washed with the new medium and then 10 μg/mL LPS was added to the culture medium. After 24 h, cells were collected for further analyses.

Cell proliferation assay

Cell viability assays were performed according to the Cell Counting Kit-8 (CCK-8) guide (Solarbio, Beijing, China) guide. HC11 and RAW264.7 cells were seeded in 96-well plates at a density of 1×10^3 and incubated overnight at 37℃. Cells were treated with various concentrations of Colo EVs with DMEM for 24 h. Then, 10 μL of CCK8 solution was added to the media. Absorbance at 450 nm was detected on a microplate reader (CMax Plus, Molecular Devices, China).

Cell proliferation rate was calculated using the following equation: cell proliferation rate (%) = (An − Ac)/ (A0 -Ac) × 100 (%), in which "An" is the absorbance value of cells with various concentrations of Colo EVs at 24 h, "A0" is the absorbance value of cells cultured without Colo EVs, and "Ac" is the absorbance value of CCK-8 solution and culture media.

Cell scratch assay

HC11 (mouse mammary epithelium cells) were cultured in 6-well plates, and when cells reached 90% confluence, a straight line was scratched using a sterile 200 μL pipette

tip. Then, cells were treated with EVs (≈2×10^9 particles/mL) and cultured in FBS-free DMEM for 24 h. Images of the narrow wound-like gaps were captured by an inverted microscope (Eclipse TS100, Nikon, Japan) and analyzed. Briefly, the area of the scratch wound was measured at 0 h, 6 h, 12 h, and 24 h. The wound closure rate was calculated by comparing the area at each time point to the initial one with ImageJ software (NIH, USA).

Animal treatment and tissue sample collection

All experimental procedures in the study and the care of experimental animals were followed in conformity with the Manual of Care and Use of Laboratory Animals published by the National Institutes of Health. Pregnant female BALB/c mice (6 to 8 wk old, $n=24$) were purchased from SPF Biotechnology Co., Ltd and housed in the laboratory animal room at the Experimental Animal Center of China Agricultural University, with *ad libitum* access to commercial mouse feed and drinking water.

The test was performed 5 d after parturition. Mouse pups were separated from the female mice and the latter were randomly and equally allocated into 4 groups: control group (Con), LPS group (LPS), LPS+Colo EVs treatment group (Colo EVs+LPS), and only Colo EVs group (Colo EVs).

Female mice were anesthetized with Zoletil 50 (0.05 mg/kg im), restrained, and the fourth pair of nipples was sterilized with 75% alcohol. With the aid of a stereomicroscope, the distal end of the nipple was excised with iris scissors and then liquid was slowly injected into the mammary gland with a micro-syringe and a 33-gauge blunt needle. For the LPS and LPS+Colo EVs treatment groups, 50 μL of LPS (0.5 mg/mL) per nipple was infused into the fourth pair of mammary glands through the teat canals, whereas for the control group, the same volume of PBS was injected. After 30 min, 120 μg of Colo EVs were subcutaneously injected into the base of the fourth-pair mammary gland, according to the experimental design. For both treatments, the control group was given an injection of the same volume of PBS. After mice had fully recovered, they were placed in breeding cages and allowed access to mouse feed and water.

At 24 h after injection, mice were euthanized with pentobarbital sodium (100 mg/kg im) and mammary glands were collected.

Histological analyses

Mouse mammary glands were fixed in 4% paraformaldehyde, embedded in paraffin and sliced into 5 μm thick sections for hematoxylin and eosin (H&E) staining. Images of stained sections were captured with a light microscope.

After dewaxing and dehydrating paraffin-embedded sections of murine mammary gland tissue, primary antibody (ZO-1, Occludin, or Claudin-3) with a 1:500 dilution was exposed to the tissue section and incubated at 4 °C overnight. The tissue section was washed 3 times with PBS, secondary antibody (goat anti-rabbit-HRP) with a 1:200 dilution was added and incubated at room temperature for 1 h. Hematoxylin was used to stain nuclei, the section was dehydrated with increasing concentrations of alcohol, and finally it was sealed with neutral gum.

Histological analysis of mammary glands was performed to evaluate overall inflammation. Severity was scored based on criteria reported by Gogio-Tiwari et al. [21] and data reported in Supplementary file Table S1.

Protein concentrations of TNF-α, IL-6, IL-1β and myeloperoxidase

Excised mammary glands were cut into small pieces and 0.1 g tissue was homogenized in 1 mL PBS buffer. Protein concentrations of TNF-α (ml002095, Mlbio, China), IL-6 (ml098430, Mlbio, China), IL-1β (ml301814, Mlbio, China), and MPO (Myeloperoxidase, ml002070, Mlbio, China) in mammary glands were assessed using mouse enzyme-linked immunosorbent assay (ELISA) kits, according to the manufacturer's instructions. Absorbance at 450 nm was detected on a microplate reader (CMax Plus, Molecular Devices, China).

Transcriptome of tissue samples

A total of 11 murine mammary gland tissue samples were sent for RNA sequencing (RNA-seq) analysis, comprised of 3 from the CON group, 4 from the LPS group, and 4 from the Colo EVs+LPS group. A standard procedure of RNA sequencing was conducted on a BHI sequencer by OE Biotech Co., Ltd. (Shanghai, China). Expression levels of transcripts were calculated using the transcripts per million reads method. The analysis was conducted by R programming using the DESeq package, including standardization, calculating multiple differences, and assessing significance of differences in reads. DEGs ($|FC| > 1.5$ and p-adjusted < 0.05) were considered significant. The Venn plot, principal component analysis (PCA) plot, volcano plot, heatmap, and PPI plot were generated using a free online platform (https://cloud.oebiotech.com/).

RNA extraction, cDNA synthesis, and quantitative real-time PCR (qPCR)

Total RNA was extracted using the RNA-easy Isolation Reagent (Vazyme, Nanjing, China) according to the manufacturer's instruction. Briefly, 0.05 g homogenate mouse mammary gland tissue or a single well of cell culture was lysed with 1 mL RNA-easy Isolation Reagent in a centrifuge tube to release RNA and denature proteins. After 0.2 mL dilution buffer was added to the lysate, the extraction process was performed under centrifugation. Then, RNA

was washed twice with 75% ethanol prepared with RNA-ase-free ddH_2O twice, the RNA pellet was dissolved and vortexed at room temperature, and RNA was quantified using Nanodrop (Thermo Fisher Scientific, CA, USA).

cDNA synthesis was performed using HiScript® III 1st Strand cDNA Synthesis Kit (Vazyme, NanjingChina) according to instructions. The qPCR reaction was performed on an ABI 7500 using SYBR mix and the ΔΔCT method used to calculate the relative expression of mRNA. The primer used is in Supplementary File Table S2.

Western blotting

Whole-cell lysates were prepared by washing cells with PBS, pelleting, and then lysing with radioimmunoprecipitation assay (RIPA) buffer. Colo EVs were mixed with the same volume of RIPA for further use. Protein concentrations of samples were qualified using a BCA assay (CWBIO, China), and protein was denatured with SDS-PAGE loading buffer (Beyond Times, China), with 10% Sodium dodecyl sulfate (SDS) polyargyrite gel used to separate proteins. For this, 35 μg protein was added into each well, proteins were transferred to ta 0.22 μm PVDF membrane and blocked with 5% skimmed milk for 2 h. Primary antibodies were bound to target protein for 12 h. The membrane was rinsed with Tris-buffered saline and 0.1% Tween 20 detergent (TBST) and proteins were marked as incubated with the HRP-labeled secondary antibody for 60 min at room temperature. After washing with Tris-buffered saline, the membrane was developed using ECL reagents and visualized with a chemiluminescence system (Tannon, China). We used the following antibodies: TSG101 (ABclonal, China, A1692, 1:1000), CD81 (ABclonal, China, A5270, 1:1000), Calnexin (ABclonal, China, A15631, 1:1000), HSP70 (Abmart, China, T55496, 1:1000), ZO-1 (Huabio, China, ER41204, 1:1000), Occludin (Huabio, China, R1510-33, 1:1000), Claudin-3 (ABclonal, China, A24603, 1:1000), COX-2 (Huabio, China, RT1159, 1:1000), INOS (Abmart, China, TA0199, 1:1000), Phospho-IκB alpha(S32) (Huabio, China, ET1609-78, 1:1000), Phospho-NF-κB p65 (S529) (Huabio, China, ET1604-27, 1:1000), NF-κB p65 (Cell Signaling Technology, USA, 6956T,1:1000), IκBα (Cell Signaling Technology, USA, 4812 S,1:1000), β-Actin (Proteintech, China, 81115-1-RR,1:1000), HRP-conjugated Affinipure Goat Anti-Mouse IgG(H+L) (Proteintech, China, SA00001-1,1:20000), HRP-conjugated Affinipure Goat Anti-Rabbit IgG(H+L) (Proteintech, China, SA00001-2,1:20000).

Immunofluorescence staining

HC11 were cultured on a unique detachable chamber of a sterile Nunc Lab-Tek chamber slide system prior to staining and were fixed with 4% paraformaldehyde for 20 min. After three PBS washes, 5 min each time, the slides were permeabilized for 5 min at 4 °C with 0.2% Triton X-100 in PBS. Following by blocked for 1 h in 5% goat serum at 4 °C, HC11 were incubated with antibodies mentioned above ZO-1(1:1000), Occludin(1:1000) and Claudin-3(1:1000) overnight at 4 ℃. After washed gently with PBS, cells were incubated with CoraLite488-conjugated AffiniPure goat anti-rabbit IgG (H+L) in the dark for 1 h, and stained with 500 μL DAPI for 10 min. Immunofluorescence was visualized under a confocal laser-scanning microscope (NIKON, Japan).

Statistical analyses

Quantitative data are expressed as the mean±standard deviation (SD). Statistical analyses were performed using GraphPad Prism 9 software. The statistical significance of the differences between groups was determined by non-parametric Mann-Whitney test and $p<0.05$ was considered significant. All data were obtained from at least 3 biological replicates, and "n" represents the number of independent samples for each group.

Results

Isolation and characterization of Colo EVs

To evaluate whether Colo EVs were properly isolated, a variety of methods were used in strict adherence to the Minimal Information Guidelines for Extracellular Vesicles Studies (MISEV2018) [22]. Extracted Colo EVs were characterized by size, morphology, and protein markers. In this study, transmission electron microscopy was used to determine the morphology of Colo EVs, and the typical spherical shape and lipid bilayer were in the captured images (Fig. 1A). Western blot analysis revealed that these Colo EVs expressed classical EV biomarkers: Heat shock protein 70 (HSP70), ESCRT-associated proteins (TSG101), and Tetraspanins (CD81) but did not express endoplasmic reticulum marker (calnexin). (Fig. 1B). The supernatant was used as a negative control in the western blot and showed a band for calnexin only at a high protein concentration (40 μg) (Supplementary Figure S1). The median size of Colo EVs was 149.6 nm (range of 88.5–239.0 nm; Fig. 2C). Every milliliter of bovine colostrum yielded approximately 4.3×10^{11} particles and 3.4 mg of protein in Colo EVs.

Colo EVs promoted cell proliferation and migration *in vitro*

Cell proliferation assays were conducted using HC11 (mouse mammary epithelium cells) and RAW264.7 (mouse monocyte macrophages) cell lines to investigate effects of Colo EVs on cell proliferation. Colo EVs were added to the cells at various concentrations, and cell proliferation was assessed using the CCK-8 assay. There was a significant increase in cell proliferation in both HC11 and RAW264.7 cell lines following treatment with

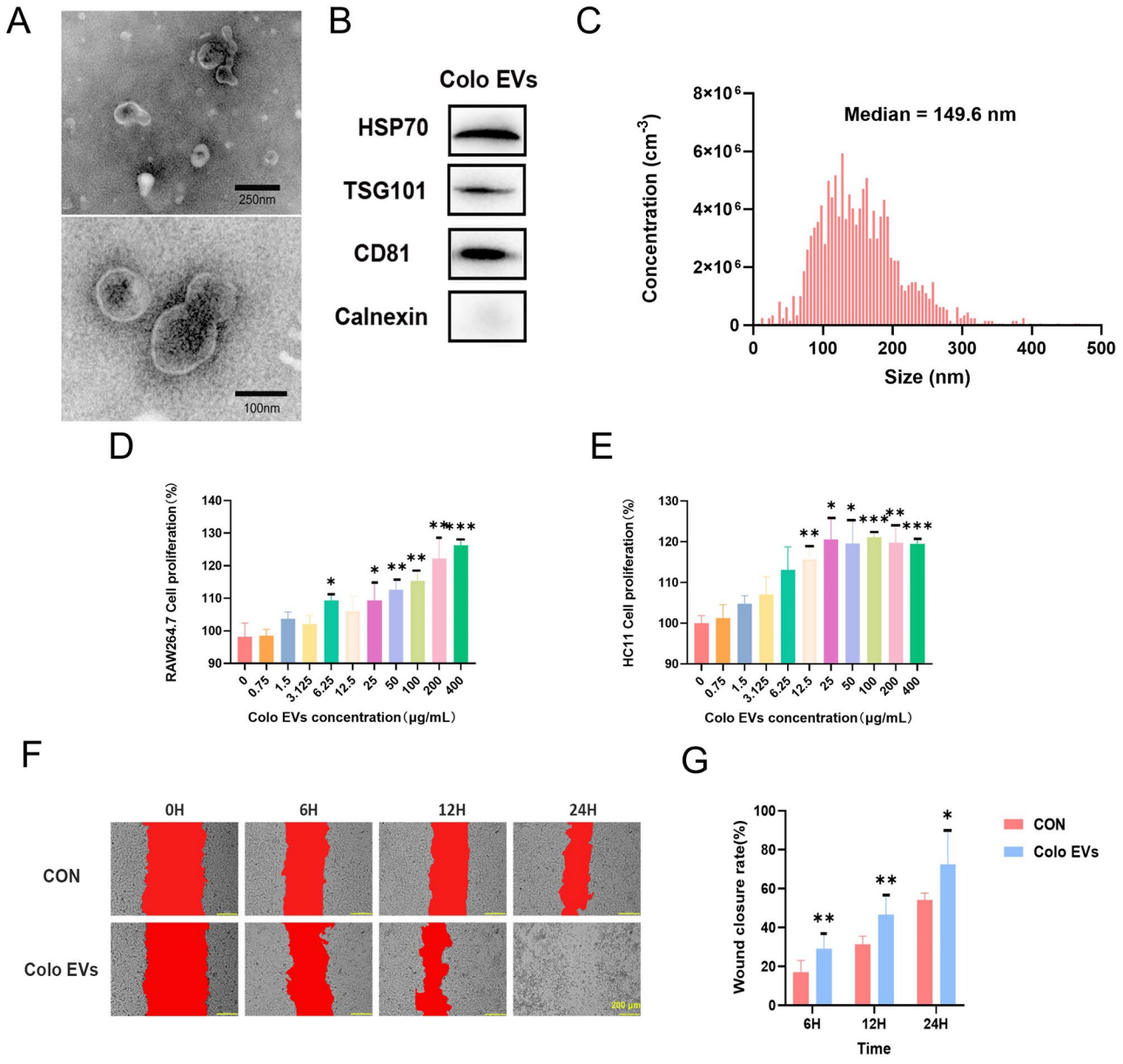

Fig. 1 Evaluation of the production parameters and bioproperties of Colo EVs. (**A**) Morphological analysis of Colo EVs by TEM. (**B**) Western blot analysis of Colo EVs protein markers. (**C**) The size distribution of Colo EVs by NTA. (**D**) The effect of Colo EVs on RAW264.7 cell proliferation. (**E**) The effect of Colo EVs on HC11 cell proliferation. (**F**) Representative cell migration images of HC11 cells after Colo EVs treatment (scale bar = 200 μm). The red color indicates the scratch wound. (**G**) Quantification of the cell migration ratio in each group ($n = 3$). *$p < 0.05$, **$p < 0.01$

Colo EVs. Importantly, Colo EVs did not exhibit toxicity towards either cell line (Fig. 1D and E).

Effects of Colo EVs on cell migration ability were assessed using scratch assays with HC11. Upon addition of Colo EVs, migration rates increased by almost 80% compared to control conditions (Fig. 1F and G). Therefore, Colo EVs had good biocompatibility and promoted cell proliferation and migration *in vitro*.

Colo EVs reduced LPS-induced inflammatory response *in vitro* in mouse monocyte macrophages (RAW264.7)

As a classic culture model of inflammatory disease, LPS-induced RAW264.7 has been extensively used to identify potential treatment agents for various inflammation-related syndromes [23]. This cell model was used to assess anti-inflammatory properties of Colo EVs.

Firstly, gene expression of proinflammatory cytokines IL-6, TNF-α, and IL-1β were analyzed using qPCR. Stimulation with LPS significantly increased mRNA expression in RAW264. However, pretreatment with Colo EVs

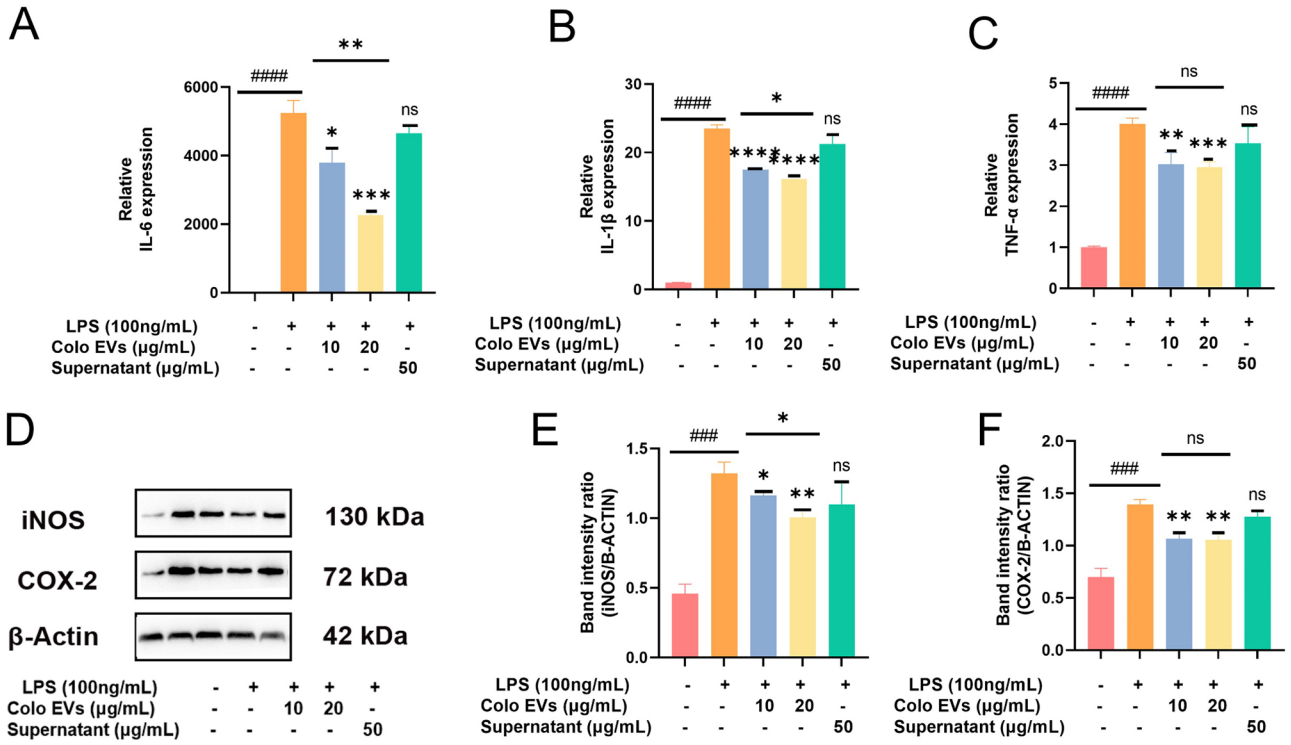

Fig. 2 Colo EVs reduced inflammatory response on LPS-induced RAW264.7 (**A**–**C**) Effect of Colo EVs and supernatant on the mRNA expression of IL-6, IL-1β, and TNF-α in LPS-stimulated RAW264.7 cells. (**D**) Effect of Colo EVs and supernatant on protein concentration of iNOS and COX-2. (**E**, **F**) Densitometric analysis of the effects of Colo EVs on iNOS and COX-2 expression. Proteins were analyzed by western blotting; β-actin served as an internal control. ###$p < 0.001$, ####$p < 0.0001$, versus CON. *$p < 0.05$, **$p < 0.01$, ***$p < 0.001$, ****$p < 0.0001$, * versus LPS

successfully attenuated cytokine expression at the RNA level, with dose-dependent effects, especially for IL-6 and IL-1β. However, supernatant from the isolation process, used as a control, did not significantly reduce inflammatory cytokine expression (Fig. 2A, B and C).

Protein concentrations of iNOS and COX-2 were assessed with western blot analysis. Similar to the gene expression results, LPS induced a significant increase in these inflammatory enzymes, whereas Colo EVs decreased their upregulated protein expression. The supernatan group was not significantly different from the LPS group. (Figure 2D, E and F)

Severe inflammatory response and tissue damage contributed to mastitis

In line with previous studies [24], we established and examined a murine model of mastitis (Fig. 3A). At 1 d after the LPS injection, there was congestion and swelling of the fourth pair of mammary glands (Fig. 3B). In addition, mRNA expression of pro-inflammatory cytokines (IL-6, IL-1β) was markedly increased in the LPS group, consistent with an intense inflammatory response (Fig. 3C). Likewise, the hematoxylin-eosin staining (H&E) staining of the mammary tissue section of LPS group revealed extensive neutrophil infiltration. Some of heavily affected alveoli had shedding of epithelial cells and disrupted mammary acinar structure (Fig. 3D). Overall, the inflammation score was significantly higher in the LPS group compared to the control (Fig. 3E). The LPS-induced murine mastitis caused a profound inflammatory response and structural damage, providing a suitable model to evaluate mastitis treatments.

Colo EVs attenuated LPS-induced murine mastitis

A murine mastitis model was used to test the effect of Colo EVs on mastitis. An overview is in Fig. 4A. Based on clinical observations, mice in the LPS group had redness mammary glands, indicative of inflammation, whereas these effects were attenuated in the Colo EVs treatment group. Mice that received only Colo EVs did not show severe color changes compared to the CON group (Fig. 4B).

Histological analysis further supported these observations. The images from LPS group demonstrated a severe inflammation response characterized by the intensive neutrophil infiltration into the luminal space. In some heavily affected acini, the epithelial lining was disrupted and the alveolar structure was abnormal. However, in Colo EVs+LPS group the number of neutrophils was observed to be reduced with relatively normal alveolar, suggesting that the inflammatory response induced by LPS was significantly mitigated. The Colo EVs group

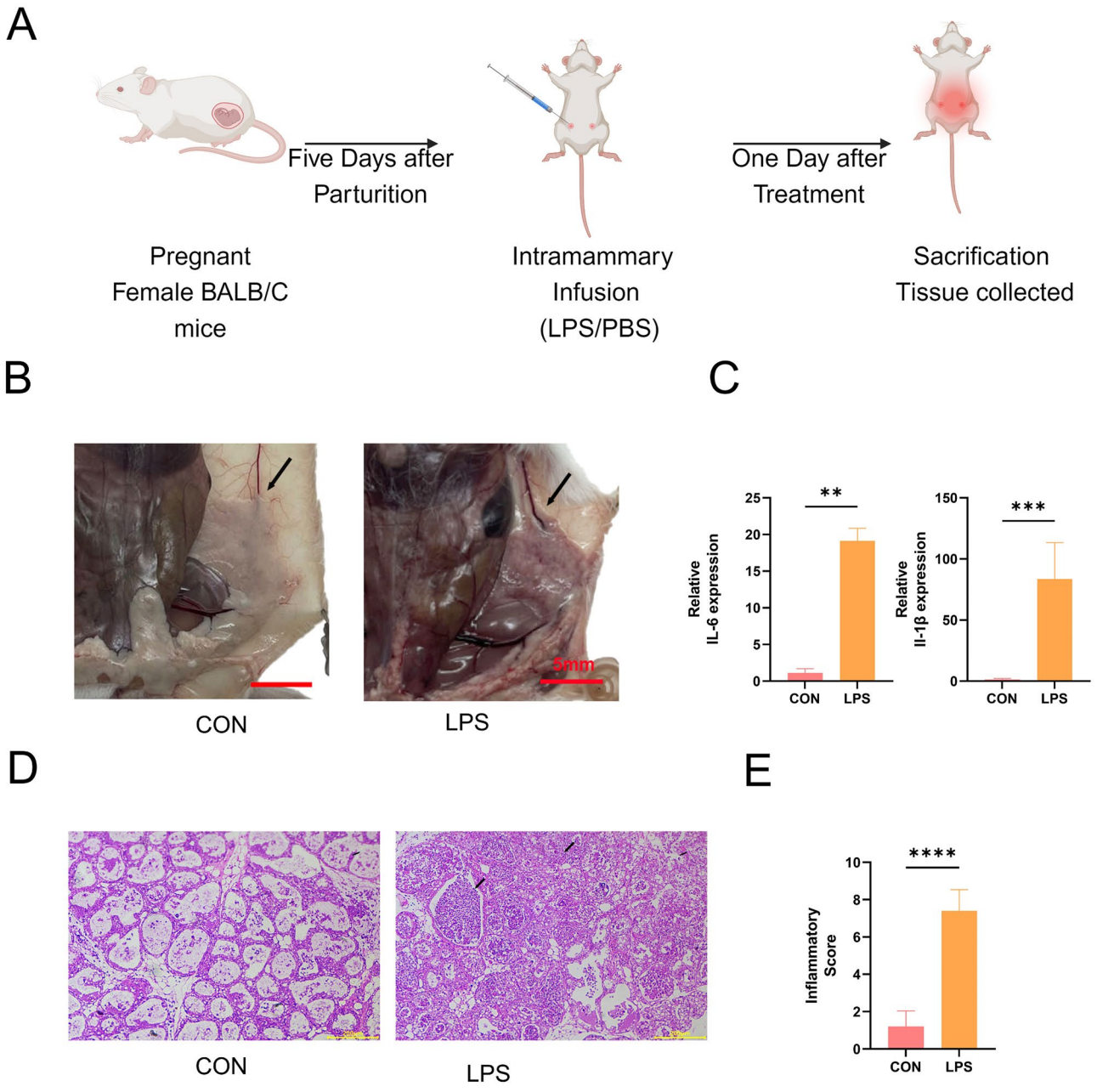

Fig. 3 Pathological changes of LPS-induced Murine mastitis. (**A**) Experimental scheme of murine mastitis. (**B**) Representative image of gross pathological features in control and LPS groups. Arrows indicate the location of the mammary gland. (**C**) The Relative expression of pro-inflammatory cytokine IL-6, and IL-1β. (**D**) Representative images of mammary gland H&E staining, arrows indicating neutrophil infiltration, and damaged alveolar structure. (**E**) inflammatory scores of two groups. $^{**}p < 0.01$, $^{***}p < 0.001$, $^{****}p < 0.0001$

showed few leukocyte infiltrations, with overall counts similar to the CON group (Fig. 4C). Overall inflammatory scores indicated significant improvement in the Colo EVs+LPS group compared to the LPS group, while the Colo EVs group did not show significant changes compared to the CON group. (Fig. 4D).

Expression levels of pro-inflammatory markers IL-1β, IL-6, TNF-α, and inflammatory enzyme MPO in mammary gland tissue homogenates were significantly increased in the LPS group compared to the control group. However, Colo EVs treatment suppressed expression of these inflammatory mediators, suggesting a protective effect against LPS-induced inflammation. For those that received only Colo EVs treatment, only IL-6 was significantly higher than in the CON group, while other proteins did not show a statistical difference(Fig. 5A, B, C and D).

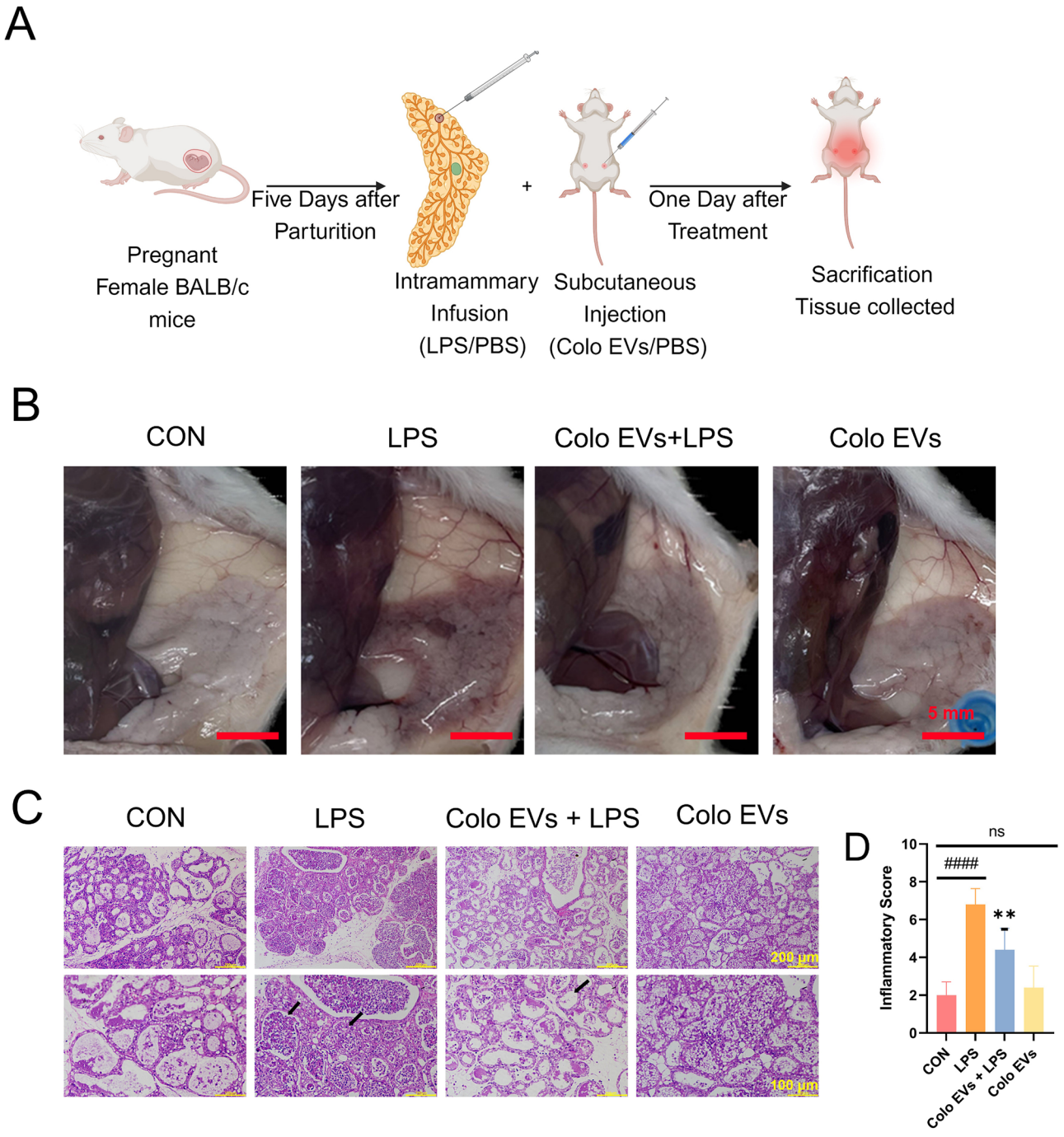

Fig. 4 Colo EVs attenuated LPS-induced murine mastitis. (**A**) Experimental scheme of treatments. (**B**) Representative images of the gross pathological feature in murine mammary glands with LPS, Colo EVs treatment. (**C**) Representative images of mammary glands H&E staining. Arrows in LPS group image indicated severe neutrophil infiltration and disrupted alveolus structure, respectively. The arrow in Colo EVs indicated intact mammary alveoli. (**D**) Inflammatory score of Murine mammary glands. ####$p<0.0001$, #versus CON. **$p<0.01$, *versus LPS

Colo EVs protected the BMB from LPS challenge *in vivo*

The increase in mammary leukocyte infiltration and inflammation is attributed to the impaired integrity of BMB [25]. Effects of Colo EVs on tight junction proteins of BMB were investigated using immunohistochemistry (IHC). In CON group, the tight junction proteins ZO-1, Occludin, and Claudin-3 were predominantly localized at the luminal region of alveolae, indicating the intergrity of the tissue. However, the LPS challenge led to a reduction in the expression of ZO-1 and Occludin evidenced by a diminished contrast between negative and positive staining. Although changes in Claudin-3 expression were not

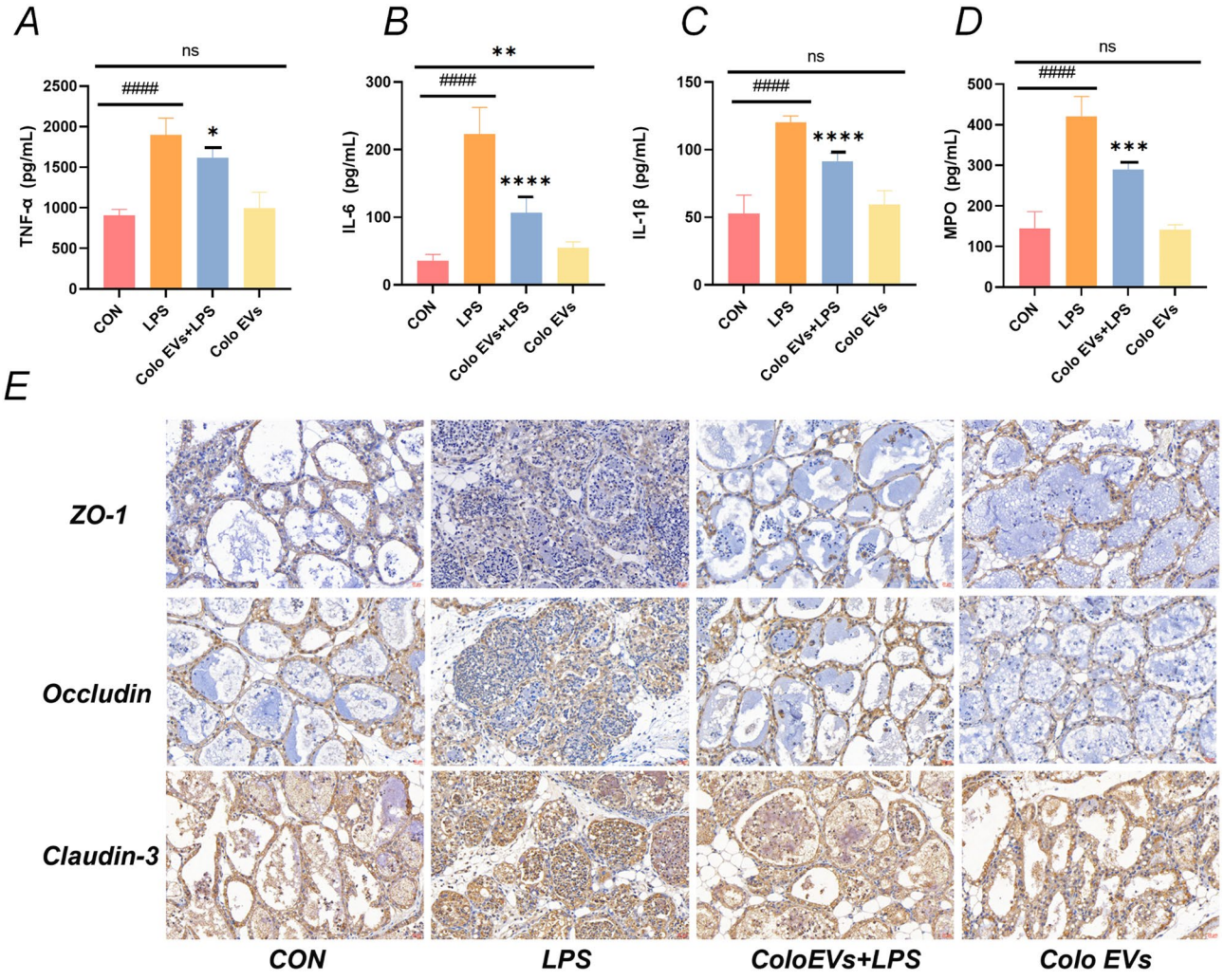

Fig. 5 Colo EVs alleviated inflammation and tight junction damage in murine mastitis. (**A**) The protein concentration of IL-6, IL-1β, TNF-α, and MPO in mammary gland. (**B**) Representative images of mammary gland immunohistochemistry for ZO-1, Occludin, and Claudin-3. ####p<0.0001, #versus CON. *p < 0.05, **p < 0.01, ***p < 0.001, ****p<0.0001, *versus LPS

clearly detectable, disorganized mammary epithelial cells in the luminal area suggested structural impairment of the tissue. Following Colo EVs treatment, the decreased expression of tight junction proteins and disrupted glandular structure were alleviated, as shown by relatively normal IHC images. In the group that only received Colo EVs, tight junction protein localization and expression were largely preserved (Fig. 5E).

Transcriptomic analysis revealed anti-inflammatory and regenerative roles of Colo EVs

In this study, RNA-seq analysis of murine mammary tissue was used to investigate effects of Colo EVs on mastitis. Principal component analysis (PCA) and heatmap analysis revealed distinct separation and altered gene expression profiles between the LPS group and Colo EVs treatment group (Fig. 6A and B). PCA analysis with separation among 3 groups and Venn graph of two comparisons (LPS vs. CON and Colo EVs vs. LPS) are in Supplementary Figure S2. In total, 446 up-regulated genes and 395 down-regulated genes were identified in the Colo EVs treatment group compared to the LPS group (Fig. 6C). Differentially expressed genes (DEGs) were predominantly enriched in inflammatory response pathways, including T-helper 2 cell differentiation, IL-1β production, and response to bacterium in GO and KEGG databases (Fig. 6D and E).

Construction of a PPI (protein-protein interaction) network was done to identify reactions between genes. Genes regulating inflammatory response were largely down-regulated (e.g., *Il6*, *Il1b*). Interestingly, genes involved in milk synthesis (e.g., *Csn3*, *Lalba*, *Glycam*) were up-regulated in the Colo EVs treatment group, indicating potential preservation of lactation function under LPS challenge. (Fig. 7A).

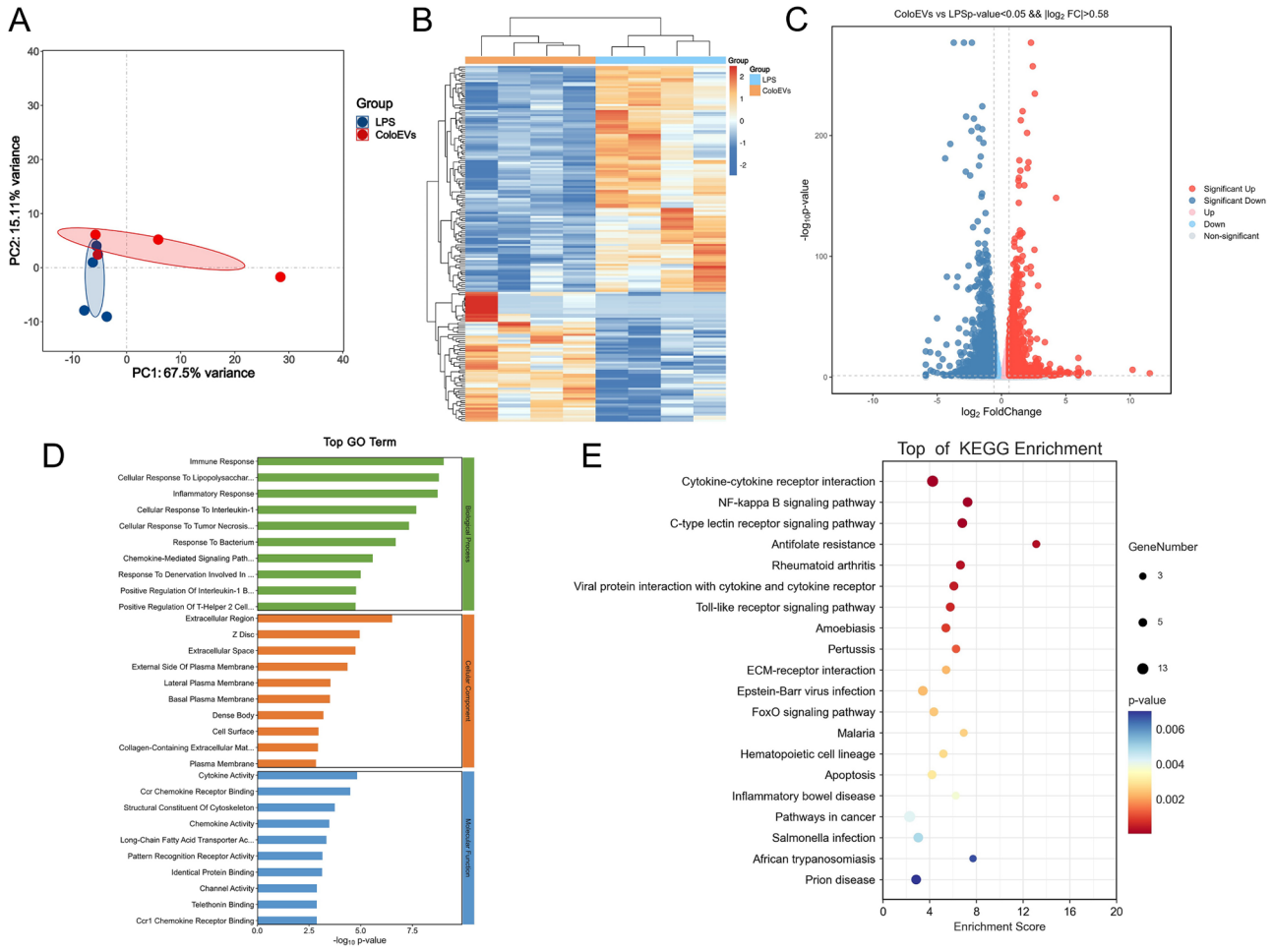

Fig. 6 Transcriptional analysis of murine mammary glands. (**A**) PCA score plot representing discrepancies among LPS group and Colo EVs + LPS group (shown as ColoEVs) (**B**). Heatmap of the DEGs ($n = 4$). (**C**) Volcano plots showing the number of DEGs between two groups (p-adjusted < 0.05 and |log-2FC|>0.58). (**D**). Top GO term enrichment of DEGs. (**E**) Top KEGG enrichments of DEGs

Some related pathways were selected to demonstrate the heatmap for visualization (Fig. 7B). Colo EVs treatment group had down-regulation of the NF-κB pathway, a central pathway regulating innate immunity and inflammatory response [20]. Also, FoxO downstream function effectors coding genes like apoptosis (*Gadd45a/b*, *Bcl2l1*) and cell cycle (*Plk2*) were downregulated. Other identified genes related to wound healing, such as Aq*p1* and *Col3a1*, were also up-regulated. Regarding upregulated genes, multiple metabolic-related genes were upregulated in the Colo EVs treatment group (*Acss1*, *Glul*), suggesting that Colo EVs could modulate inflammatory response by metabolic pathways.

To validate RNA-seq findings, qPCR analysis was done on several genes, and results were consistent with transcriptional analyses (Fig. 7C).

Colo EVs had an anti-inflammatory role through the NF-κB signaling pathway *in vitro* in LPS-challenged RAW264.7

Given the enrichment of NF-κB activation-related genes in transcriptome results, we further explored whether the NF-κB pathway mediated the Colo EVs-mediated inhibition of the inflammatory response in mastitis using RAW264.7 culture model. Protein concentrations of NF-κB subunit P65 and its inhibitor IkBα were determined by western blotting. Phosphorylation of P65 and IkBα was significantly increased after LPS treatment but was significantly reduced by Colo EVs pre-treatment in a dose-dependent trend. (Figure 8A, B and C). These results suggest that Colo EVs exert their anti-inflammatory capability by suppressing activation of the NF-κB signaling pathway.

Colo EVs protected the expression of tight junction protein *in vitro* in LPS- challenged HC11

During mastitis, disruption of the BMB leads to increased neutrophil infiltration into mammary alveoli,

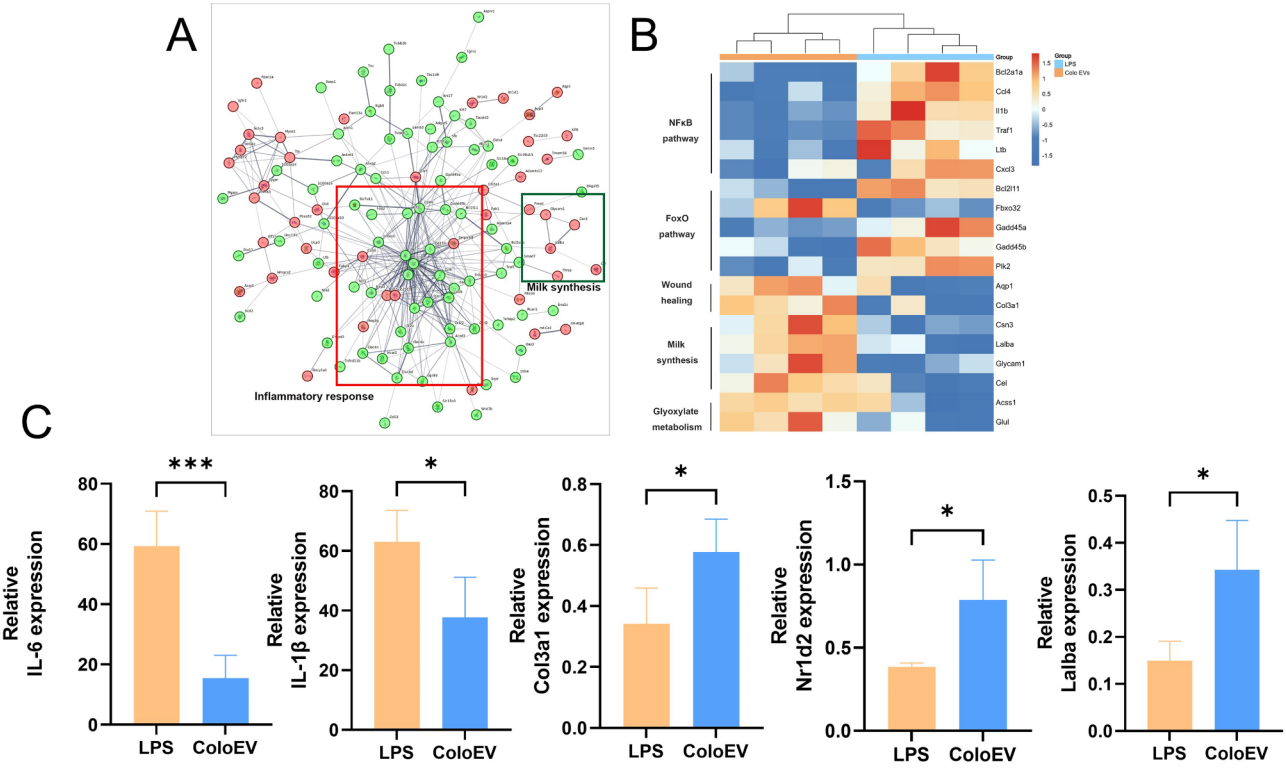

Fig. 7 Identification of key pathways of Colo EVs alleviating mastitis *in vivo*. (**A**) The predicted protein-protein interaction of DEGs. (**B**) Key genes in related pathways. (**C**) mRNA expression of IL-6, IL-1β, Col3a1, Nr1d2, and Lalba. *$p < 0.05$, ***$p < 0.001$, * versus LPS

exacerbating the inflammatory response. Maintaining the integrity of the BMB is crucial for attenuating tissue damage and inflammation during mastitis [6]. As a culture model of mammary epithelium, HC11 cells in culture dishes exhibited polygonal or spindle-shaped epithelial morphology and formed small, compact colonies, as shown in Supplementary Figure S3A. These cells expressed tight junction proteins, including ZO-1, Occludin, and Claudin-3, which were distinctly localized at the intercellular junctions, as seen in Supplementary Figure S3B. In the present study, tight junction proteins, crucial components of the BMB, were downregulated during LPS challenge, suggesting potential disruption of barrier integrity. However, Colo EVs mitigated this effect by protecting tight junction expression. Specifically, Colo EVs prevented the downregulation of tight junction proteins ZO-1, Occludin, and Claudin-3 in mouse mammary epithelium cells HC11 challenged with LPS(Fig. 8D 8E, 8F).

Discussion

In this study, Colo EVs isolated in our provided method demonstrated good therapeutic effects and biocompatibility both *in vivo* and *in vitro* on LPS-induced mastitis models. Colo EVs treatment largely attenuated symptoms of acute mastitis by decreasing cytokine expression and neutrophil infiltration, protecting mammary alveoli, and reducing inflammatory scores. In addition, mice injected with only Colo EVs did not have a significant inflammatory response, indicating that Colo EVs have good biocompatibility. Macrophages, as innate immune cells, also have an indispensable role in mastitis by releasing TNF- α, and IL-1β to promote neutrophil infiltration into mammary alveoli during the onset of mastitis [4]. Consistent with experiments *in vivo*, Colo EVs reduced the expression of pro-inflammatory factors induced by LPS in mouse monocyte macrophages. Also, expression levels of pro-inflammatory enzymes, iNOS, and COX-2, in RAW264.7 cells were decreased by Colo EVs. iNOS can induce production of a large amount of NO, mediate and promote occurrence and development of inflammatory diseases [26], whereas COX-2 can catalyze the conversion of arachidonic acid to prostaglandins and participate in NF-κB signaling pathway activation [27]. In addition, NF-κB, a core signal pathway involved in the inflammatory response, was upregulated in multiple diseases [28]. In our study, both *in vivo* and *in vitro* evidence demonstrated that the NF-κB signaling pathway was downregulated by Colo EVs treatment, suggesting that this pathway is one of the underlying mechanisms through which Colo EVs exert their anti-inflammatory effects.

The BMB is an important component of innate immunity of the mammary gland, relying on the integrity of epithelial cells and their synergistic implementation with intercellular connections [6]. Tight junction proteins

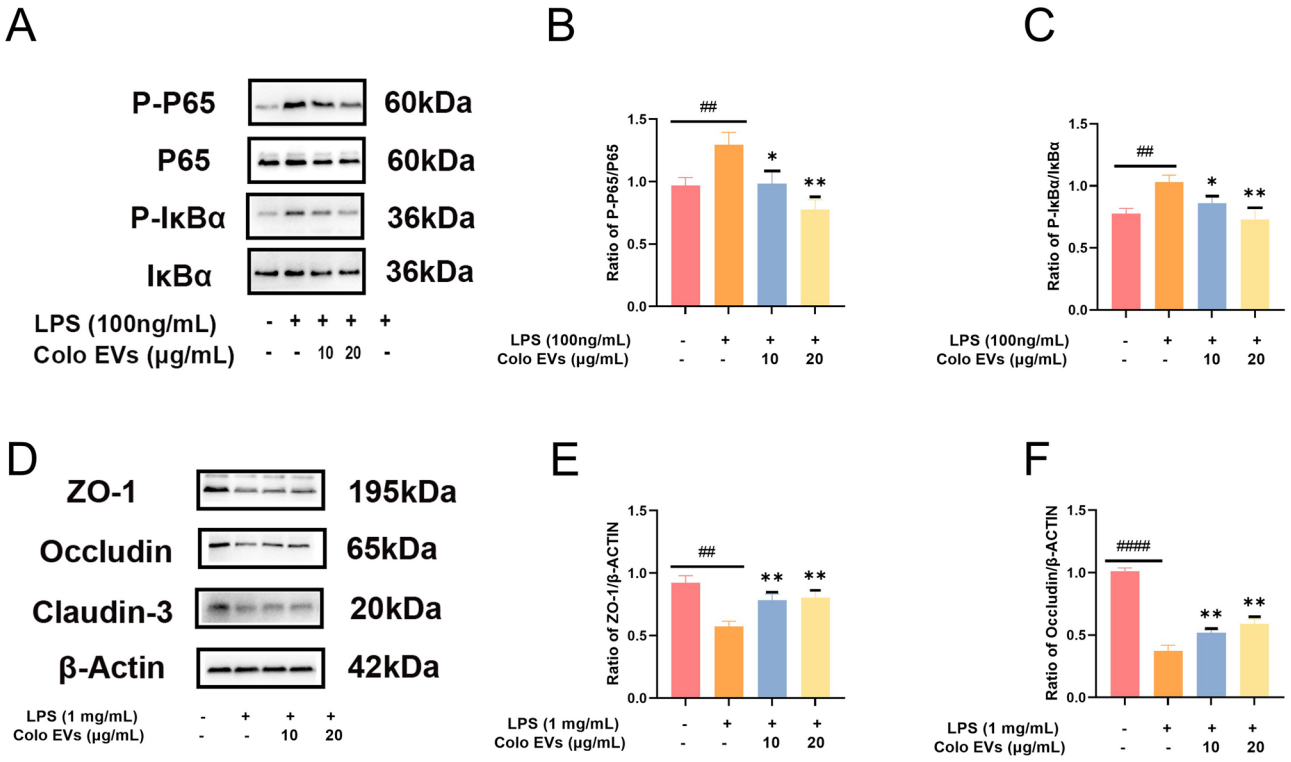

Fig. 8 Colo EVs suppress the activation of NF-κB pathway and restore tight junction protein expression *in vitro*. (**A**) Effect of Colo EVs the on phosphorylation of key proteins, P65 and IKBα, in NF-κB signal pathway activation in RAW264.7 cells. (**B**, **C**) Densitometric analysis of NF-κB p65 and IκBα phosphorylation in RAW264.7 cells. (**D**) Effect of Colo EVs on tight junction proteins, ZO-1, Occludin, Claudin-3 in HC11. (**E**, **F**) Densitometric analysis of ZO-1 and Occludin expression. Proteins were analyzed by western blotting; β-actin served as an internal control in HC11. Images are representative of three independent experiments. ##$p < 0.01$, ####$p < 0.0001$, # verses CON. *$p < 0.05$, **$p < 0.01$, * versus LPS

(ZO-1, claudin-3, and Occludin) role are important in maintaining BMB function, with Colo EVs protecting expression of tight junction proteins and BMB integrity. In transcriptome analysis, related genes regulating milk secretion were up-regulated compared to LPS group, which further reflected that Colo EVs have the potential of protecting the secretory function of mammary glands. Furthermore, DEGs were enriched in the FoxO signaling pathway. FoxOs have an important role in maintaining normal cellular physiology by regulating survival, cell apoptosis, autophagy, oxidative stress, development and maturation of T and B lymphocytes, and secretion of inflammatory cytokinesis [29]. Meanwhile, FoxOs can be induced by LPS and if produced through the NF-κB signaling pathway have a synergistic role in transmission of inflammatory signals [30]. One study on the effect of selenium on MAC-T cells infected with *Staphylococcus aureus* reported a downregulated FoxO pathway at the transcriptional level with the protective effect of selenium [31]. Inhibition of the FoxO signaling pathway has benefits in several conditions, including chronic liver injury, fibrosis, and endothelial injury [32, 33]. However, the role of the FoxO pathway in mastitis has not yet been reported.

Furthermore, consistent with another study using Colo EVs as therapeutic agents but in surgical wounds [34], there was upregulation of genes involved in wound healing in the transcriptome of Colo EVs+LPS group, including *Aqp1* and *Col3a1*. The former is a small membrane transporter protein that mainly acts as a water transport pore, promoting osmotic-driven water transport across cytoplasmic membranes [35]. Involvement of Aqps in inflammatory disease has been explored due to its roles in cell migration and edema formation [36–38]. An Aqp1 deficiency hurts tissue integrity, e.g., intestinal epithelial barrier [39]. Col3a1, as a type III collagen, is an important component of the Extracellular Matrix (ECM) [40]. During mastitis, inflammation can disrupt the integrity of the ECM and cause epithelial cell death [5]. Upregulation of ECM proteins-related genes is beneficial for protecting the integrity of glandular tissue and function. Colo EVs may upregulate genes involved in tissue repair, enabling the tissue to transition from an inflammatory process to a repair process, thereby avoiding tissue damage and the functional imbalance caused by persistent and excessive inflammation.

Colo EVs contain a rich mixture of bioactive components, including growth factors, proteins, mi-RNAs, lipids, etc., conferring nutritional and immune health

benefits [17, 41]. Instead of a single substance, Colo EVs may represent a biologically active "cocktail" to exert their effects. For example, TGF-β, an immunosuppressive cytokine abundant in Colo EVs, contributes to their anti-inflammatory effect [42]. Additionally, proteins such as CD5L and clusterin in Colo EVs have important roles in resolving inflammation [36]. MicroRNAs are also important components; Colo EVs have been reported to contain a broad microRNA profile, including miR-let-7b, miR-148a, and miR-27a-3p [43], known to alleviate inflammation in various diseases [44–46]. Therefore, the anti-inflammatory effect of Colo EVs can be attributed to multiple substances within them. Besides their anti-inflammatory properties, Colo EVs also had a strong ability to protect the BMB, as in the present study. Although no current research has reported this specific effect, similar studies on colitis have illustrated Colo EVs' capability to maintain barrier integrity [47]. This effect may be due to the cargo of Colo EVs promoting cell proliferation and protecting tight junction structures, including TGF-β, miR-155, and miR-21 [42]. There are many possibilities for how the cargo of Colo EVs can contribute to alleviating LPS-induced mastitis. In other words, additional functions and mechanisms of Colo EVs in mitigating mastitis were not included in our study and need to be explored in future research.

Although Colo EVs had clear beneficial effect on LPS-induced mastitis models, the mechanism of bovine mastitis is more complex than LPS-induced inflammation. In a natural setting, factors such as pathogen-host interactions, pathogen load, and environmental influences cannot be fully replicated in the lab [48]. Specifically, while Colo EVs are composed of immunomodulatory and antibacterial substances, their effects on bovine mastitis remain largely unexplored [49]. Additionally, the incidence of mastitis is high at the beginning of lactation [50], which means intense stress for cattle and a rapidly changing immune system. Introducing Colo EVs as therapeutic agents for mastitis may be risky due to the potential for disease transmission. Since studies have compared Colo EVs from cattle with various immune responses [43], larger sample sizes of bovine colostrum need to be collected and tested to establish a standard for therapeutic development.

Conclusion

The current study demonstrated the anti-inflammatory capabilities and protective effects of Colo EVs against LPS-induced inflammation, both *in vivo* and *in vitro*. Treatment with Colo EVs effectively alleviated inflammation in murine mammary glands, as evidenced by reduced inflammation scores and decreased expression of pro-inflammatory cytokines such as IL-1β, IL-6, and TNF-α, along with the inflammation-related enzyme MPO. Furthermore, Colo EV treatment preserved expression of tight junction proteins on the BMB. Additionally, Colo EVs reduced expression of COX-2 and iNOS proteins in LPS-induced mouse monocyte macrophages and mitigated reduction in tight junction proteins Claudin-3, ZO-1, and Occludin in mouse mammary epithelium cells. Transcriptional analysis and western blotting further indicated that Colo EVs may exert their effects via the NF-κB pathway. Overall, we concluded that Colo EVs have much promise as a potential candidate for mastitis treatment.

Supplementary Information

The online version contains supplementary material available at https://doi.org/10.1186/s12951-024-02926-2.

Supplementary Material 1

Supplementary Material 2

Acknowledgements

Our ultracentrifugation work was performed at the CAB Public Instrument Platform of China Agricultural University. We thank Bio-render for providing illustration materials; the graphic abstract and animal experiment scheme were created with BioRender.com.

Author contributions

YX and TS conducted the experiments, drafted the manuscript, and prepared it for visualization. PL prepared for drawing elements and revised the manuscript. JY helped with experiment techniques. JK helped with the language checking and revised the manuscript. JL, CX, and BH had co-supervision roles and substantially revised the work. JG was primary supervisor, provided financial support, and reviewed the manuscript. All authors contributed to the manuscript revision, and read, and approved the submitted version.

Funding

This work was supported by the National Natural Science Foundation of China (32273082 and U21A20262) and the National Key Research and Development Program of China (2023YFD1801101).

Data availability

No datasets were generated or analysed during the current study.

Declarations

Competing interests

The authors declare no competing interests.

Author details

[1]Department of Clinical Veterinary Medicine, College of Veterinary Medicine, China Agricultural University, 100193 Beijing, China
[2]NHC Key Laboratory of Transplant Engineering and Immunology, Frontiers Science Center for Disease-Related Molecular Network, West China Hospital, Sichuan University, 610213 Chengdu, China
[3]Faculty of Veterinary Medicine, University of Calgary, Calgary, AB T2N 4N1, Canada

Received: 10 May 2024 / Accepted: 10 October 2024
Published online: 16 October 2024

References

1. He W, Ma S, Lei L, et al. Prevalence, etiology, and economic impact of clinical mastitis on large dairy farms in China. Vet Microbiol. 2020;242:108570. https://doi.org/10.1016/j.vetmic.2019.108570.
2. Rollin E, Dhuyvetter KC, Overton MW. The cost of clinical mastitis in the first 30 days of lactation: an economic modeling tool. Prev Vet Med. 2015;122(3):257–64. https://doi.org/10.1016/j.prevetmed.2015.11.006.
3. Mudaliar M, Tassi R, Thomas FC, et al. Mastitomics, the integrated omics of bovine milk in an experimental model of Streptococcus uberis mastitis: 2. Label-free relative quantitative proteomics. Mol Biosyst. 2016;12(9):2748–61. https://doi.org/10.1039/C6MB00290K.
4. Elazar S, Gonen E, Livneh-Kol A, Rosenshine I, Shpigel NY. Neutrophil recruitment in endotoxin-induced murine mastitis is strictly dependent on mammary alveolar macrophages. Vet Res. 2010;41(1):1–14. https://doi.org/10.1051/vetres/2009058.
5. Zhao X, Lacasse P. Mammary tissue damage during bovine mastitis: causes and control. J Anim Sci. 2008;86(13 Suppl):57–65. https://doi.org/10.2527/jas.2007-0302.
6. Wellnitz O, Bruckmaier RM. Invited review: the role of the blood–milk barrier and its manipulation for the efficacy of the mammary immune response and milk production. J Dairy Sci. 2021;104(6):6376–88. https://doi.org/10.3168/jds.2020-20029.
7. Li X, Xu C, Liang B, et al. Alternatives to antibiotics for treatment of mastitis in dairy cows. Front Vet Sci. 2023;10:1160350. https://doi.org/10.3389/fvets.2023.1160350.
8. Zhang QQ, Ying GG, Pan CG, Liu YS, Zhao JL. Comprehensive evaluation of antibiotics emission and fate in the river basins of China: source analysis, multimedia modeling, and linkage to bacterial resistance. Environ Sci Technol. 2015;49(11):6772–82. https://doi.org/10.1021/acs.est.5b00729.
9. Wu Q, Duan WZ, Chen JB, et al. Extracellular vesicles: emerging roles in developing Therapeutic Approach and Delivery Tool of Chinese Herbal Medicine for the treatment of depressive disorder. Front Pharmacol. 2022;13:843412. https://doi.org/10.3389/fphar.2022.843412.
10. Wang Y, Liu S, Li L, et al. Peritoneal M2 macrophage-derived extracellular vesicles as natural multitarget nanotherapeutics to attenuate cytokine storms after severe infections. J Controlled Release. 2022;349:118–32. https://doi.org/10.1016/j.jconrel.2022.06.063.
11. Lou P, Liu S, Wang Y, et al. Neonatal-tissue-derived extracellular vesicle therapy (NEXT): a potent strategy for Precision Regenerative Medicine. Adv Mater Deerfield Beach Fla. 2023;35(33):e2300602. https://doi.org/10.1002/adma.202300602.
12. Lv K, Wang Y, Lou P, et al. Extracellular vesicles as advanced therapeutics for the resolution of organ fibrosis: current progress and future perspectives. Front Immunol. 2022;13:1042983. https://doi.org/10.3389/fimmu.2022.1042983.
13. Adriano B, Cotto NM, Chauhan N, Jaggi M, Chauhan SC, Yallapu MM. Milk exosomes: Nature's abundant nanoplatform for theranostic applications. Bioact Mater. 2021;6(8):2479–90. https://doi.org/10.1016/j.bioactmat.2021.01.009.
14. Stelwagen K, Carpenter E, Haigh B, Hodgkinson A, Wheeler TT. Immune components of bovine colostrum and milk1. J Anim Sci. 2009;87(suppl13):3–9. https://doi.org/10.2527/jas.2008-1377.
15. Izumi H, Kosaka N, Shimizu T, Sekine K, Ochiya T, Takase M. Bovine milk contains microRNA and messenger RNA that are stable under degradative conditions. J Dairy Sci. 2012;95(9):4831–41. https://doi.org/10.3168/jds.2012-5489.
16. Santoro J, Mukhopadhya A, Oliver C, Brodkorb A, Giblin L, O'Driscoll L. An investigation of extracellular vesicles in bovine colostrum, first milk and milk over the lactation curve. Food Chem. 2023;401:134029. https://doi.org/10.1016/j.foodchem.2022.134029.
17. Han G, Cho H, Kim H, et al. Bovine colostrum derived-exosomes prevent dextran sulfate sodium-induced intestinal colitis via suppression of inflammation and oxidative stress. Biomater Sci. 2022;10(8):2076–87. https://doi.org/10.1039/d1bm01797g.
18. Harnessing the Natural Healing Power of Colostrum: Bovine Milk-Derived Extracellular Vesicles from Colostrum Facilitating the Transition from Inflammation to Tissue Regeneration for Accelerating Cutaneous Wound Healing - Kim – 2022 - Advanced Healthcare Materials - Wiley Online Library. Accessed October 25. 2022. https://doi.org/10.1002/adhm.202102027
19. Gao J, Barkema HW, Zhang L, et al. Incidence of clinical mastitis and distribution of pathogens on large Chinese dairy farms. J Dairy Sci. 2017;100(6):4797–806. https://doi.org/10.3168/jds.2016-12334.
20. Lai JL, Liu YH, Liu C, et al. Indirubin inhibits LPS-Induced inflammation via TLR4 abrogation mediated by the NF-kB and MAPK signaling pathways. Inflammation. 2017;40(1):1–12. https://doi.org/10.1007/s10753-016-0447-7.
21. Gogoi-Tiwari J, Williams V, Waryah CB, et al. Mammary gland Pathology subsequent to Acute infection with strong versus weak Biofilm forming Staphylococcus aureus bovine mastitis isolates: a pilot study using non-invasive mouse Mastitis Model. PLoS ONE. 2017;12(1):e0170668. https://doi.org/10.1371/journal.pone.0170668.
22. Théry C, Witwer KW, Aikawa E, et al. Minimal information for studies of extracellular vesicles 2018 (MISEV2018): a position statement of the International Society for Extracellular Vesicles and update of the MISEV2014 guidelines. J Extracell Vesicles. 2018;7(1):1535750. https://doi.org/10.1080/20013078.2018.1535750.
23. Ishida M, Takekuni C, Nishi K, Sugahara T. p-Synephrine suppresses inflammatory responses in lipopolysaccharide-stimulated RAW264.7 cells and alleviates systemic inflammatory response syndrome in mice. Food Funct. 2022;13(9):5229–39. https://doi.org/10.1039/D2FO00299J.
24. Wang X, Feng S, Ding N, et al. Anti-inflammatory effects of Berberine Hydrochloride in an LPS-Induced Murine Model of Mastitis. Evid Based Complement Alternat Med. 2018;2018:e5164314. https://doi.org/10.1155/2018/5164314.
25. Kobayashi K. Culture models to investigate mechanisms of milk production and blood-milk barrier in mammary epithelial cells: a review and a protocol. J Mammary Gland Biol Neoplasia. 2023;28(1):8. https://doi.org/10.1007/s10911-023-09536-y.
26. Martín MC, Martinez A, Mendoza JL, et al. Influence of the inducible nitric oxide synthase gene (NOS2A) on inflammatory bowel disease susceptibility. Immunogenetics. 2007;59(11):833–7. https://doi.org/10.1007/s00251-007-0255-1.
27. Gilroy DW, Colville-Nash PR, Willis D, Chivers J, Paul-Clark MJ, Willoughby DA. Inducible cyclooxygenase may have anti-inflammatory properties. Nat Med. 1999;5(6):698–701. https://doi.org/10.1038/9550.
28. Liu T, Zhang L, Joo D, Sun SC. NF-κB signaling in inflammation. Signal Transduct Target Ther. 2017;2:17023. https://doi.org/10.1038/sigtrans.2017.23.
29. Eijkelenboom A, Burgering BMT. FOXOs: signalling integrators for homeostasis maintenance. Nat Rev Mol Cell Biol. 2013;14(2):83–97. https://doi.org/10.1038/nrm3507.
30. Su D, Coudriet GM, Hyun Kim D, et al. FoxO1 links insulin resistance to proinflammatory cytokine IL-1beta production in macrophages. Diabetes. 2009;58(11):2624–33. https://doi.org/10.2337/db09-0232.
31. Jing H, Chen Y, Liang W, Chen M, Qiu C, Guo Myao. Effects of Selenium on MAC-T cells in bovine mastitis: Transcriptome Analysis of Exosomal mRNA interactions. Biol Trace Elem Res. 2021;199(8):2904–12. https://doi.org/10.1007/s12011-020-02439-7.
32. Feng X, Liu H, Sheng Y, et al. Yinchen gongying decoction mitigates CCl4-induced chronic liver injury and fibrosis in mice implicated in inhibition of the foxo1/TGF-β1/ Smad2/3 and YAP signaling pathways. J Ethnopharmacol Published Online March. 2024;1:117975. https://doi.org/10.1016/j.jep.2024.117975.
33. Chen L, Yin Y, Liu C, et al. Metformin alleviates bevacizumab-induced vascular endothelial injury in mice through growth differentiation factor 15 upregulation. Iran J Basic Med Sci. 2024;27(3):343–51. https://doi.org/10.22038/IJBMS.2023.72759.15827.
34. Kim H, Kim DE, Han G, et al. Harnessing the Natural Healing Power of Colostrum: bovine milk-derived extracellular vesicles from Colostrum facilitating the transition from inflammation to tissue regeneration for accelerating Cutaneous Wound Healing. Adv Healthc Mater. 2022;11(6):2102027. https://doi.org/10.1002/adhm.202102027.
35. Agre P, King LS, Yasui M, et al. Aquaporin water channels–from atomic structure to clinical medicine. J Physiol. 2002;542(Pt 1):3–16. https://doi.org/10.1113/jphysiol.2002.020818.
36. Zhang J, Ma B. Alpinetin alleviates LPS-induced lung epithelial cell injury by inhibiting p38 and ERK1/2 signaling via aquaporin-1. Tissue Cell. 2024;87:102305. https://doi.org/10.1016/j.tice.2024.102305.
37. Ruiz-Ederra J, Verkman AS. Aquaporin-1-facilitated keratocyte migration in cell culture and in vivo corneal wound healing models. Exp Eye Res. 2009;89(2):159–65. https://doi.org/10.1016/j.exer.2009.03.002.
38. Saadoun S, Papadopoulos MC, Hara-Chikuma M, Verkman AS. Impairment of angiogenesis and cell migration by targeted aquaporin-1 gene disruption. Nature. 2005;434(7034):786–92. https://doi.org/10.1038/nature03460.

39. Zhao Y, Hu ZY, Lou M, et al. AQP1 Deficiency drives Phthalate-Induced Epithelial Barrier disruption through intestinal inflammation. J Agric Food Chem Published Online June. 2024;25. https://doi.org/10.1021/acs.jafc.4c03764.
40. Xue M, Jackson CJ. Extracellular matrix reorganization during Wound Healing and its impact on abnormal scarring. Adv Wound Care. 2015;4(3):119–36. https://doi.org/10.1089/wound.2013.0485.
41. Samuel M, Chisanga D, Liem M, et al. Bovine milk-derived exosomes from colostrum are enriched with proteins implicated in immune response and growth. Sci Rep. 2017;7(1):5933. https://doi.org/10.1038/s41598-017-06288-8.
42. Aarts J, Boleij A, Pieters BCH, et al. Flood Control: how milk-derived extracellular vesicles can help to improve the intestinal barrier function and Break the gut–joint Axis in Rheumatoid Arthritis. Front Immunol. 2021;12. https://doi.org/10.3389/fimmu.2021.703277.
43. Ma T, Li W, Chen Y, et al. Assessment of microRNA profiles in small extracellular vesicles isolated from bovine colostrum with different immunoglobulin G concentrations. JDS Commun. 2022;3(5):328–33. https://doi.org/10.3168/jdsc.2022-0225.
44. Chen L, Lu Q, Chen J, Feng R, Yang C. Upregulating miR-27a-3p inhibits cell proliferation and inflammation of rheumatoid arthritis synovial fibroblasts through targeting toll-like receptor 5. Exp Ther Med. 2021;22(5):1227. https://doi.org/10.3892/etm.2021.10661.
45. Anastasio C, Donisi I, Colloca A, D'Onofrio N, Balestrieri ML. MiR-148a-3p/SIRT7 Axis relieves inflammatory-Induced endothelial dysfunction. Int J Mol Sci. 2024;25(10):5087. https://doi.org/10.3390/ijms25105087.
46. Mandolesi G, Rizzo FR, Balletta S, et al. The microRNA let-7b-5p is negatively Associated with inflammation and disease severity in multiple sclerosis. Cells. 2021;10(2):330. https://doi.org/10.3390/cells10020330.
47. Mun D, Kang M, Shin M, et al. Alleviation of DSS-induced colitis via bovine colostrum-derived extracellular vesicles with microRNA let-7a-5p is mediated by regulating Akkermansia and β-hydroxybutyrate in gut environments. Microbiol Spectr. 2023;11(6):e00121–23. https://doi.org/10.1128/spectrum.00121-23.
48. Ashraf A, Imran M. Causes, types, etiological agents, prevalence, diagnosis, treatment, prevention, effects on human health and future aspects of bovine mastitis. Anim Health Res Rev. 2020;21(1):36–49. https://doi.org/10.1017/S1466252319000094.
49. Ahn G, Shin WR, Lee S, et al. Bovine Colostrum exosomes are a Promising Natural Bacteriostatic Agent against Staphylococcus aureus. ACS Infect Dis. 2023;9(4):993–1003. https://doi.org/10.1021/acsinfecdis.3c00022.
50. Chen S, Zhang H, Zhai J, Wang H, Chen X, Qi Y. Prevalence of clinical mastitis and its associated risk factors among dairy cattle in mainland China during 1982–2022: a systematic review and meta-analysis. Front Vet Sci. 2023;10. https://doi.org/10.3389/fvets.2023.1185995.

Publisher's note